Vacuum 99 (2014) 119–123

Contents lists available at SciVerse ScienceDirect

Vacuum

journal homepage: www.elsevier.com/locate/vacuum

Rapid communication

Fine-lamellar structured thermal barrier coatings fabricated by high efficiency supersonic atmospheric plasma spraying

Y. Bai [a,b,*], L. Zhao [a], K. Liu [a], J.J. Tang [a], Z.H. Han [a,*]

[a] *State Key Laboratory for Mechanical Behavior of Materials, Xi'an Jiaotong University, Xi'an 710049, PR China*
[b] *School of Mechanical Engineering, Xi'an Jiaotong University, Xi'an 710049, PR China*

ARTICLE INFO

Article history:
Received 27 March 2013
Received in revised form
9 May 2013
Accepted 13 May 2013

Keywords:
Supersonic atmospheric plasma spraying
Thermal barrier coatings
Bonding strength
Fracture toughness
Thermal cycling lives

ABSTRACT

In this work, fine-lamellar structured thermal barrier coatings (TBCs) were deposited by high efficiency supersonic atmospheric plasma spraying (SAPS). The microstructure and mechanical properties of coatings were studied. It was found that the fracture toughness and bonding strength of as-sprayed coatings were as high as 3.7 ± 0.4 MPa $m^{1/2}$ and 52 ± 4 MPa, respectively. Due to the low porosity, well-adhered fine lamellar structures, high fracture toughness and high bonding strength, the SAPS-coatings exhibited higher thermal cycling lives and only 12% coating area spalled after 390 thermal cycles, which consisted of a directly inserting samples to 1100 °C and then 5 min holding and water quenching (20–30 °C). Compared with the reported works from other researchers, the thermal cycling lives of SAPS-coatings were greatly increased. The SAPS method is believed to be a good choice to deposit TBCs with high performance and reliability.

Thermal barrier coatings (TBCs) enable modern gas-turbine engines to operate at gas temperatures well above the melting temperature of the Ni-based superalloy (1300 °C), thereby improving engine efficiency and performance [1]. The TBC system generally is composed of a ceramic Y_2O_3 partially stabilized ZrO_2 (YSZ) top coat (TC) and a metallic bond coat (BC), usually MCrAlY, where M is usually nickel, cobalt, or combination of these two. To date, the top coat is usually prepared by atmospheric plasma spraying (APS) or electron beam physical vapor deposition (EB-PVD) [2–4]. Compared with EB-PVD, APS is a low-cost method. However, the porous and micro-cracked structure of plasma sprayed coating can lead to the premature failure of TBCs at the elevated temperature [1,5]. Therefore, one effective way to enhance the thermal durability of TBCs is to decrease the number of defects and improve the cohesion and adhesion of coating, which needs to explore the new plasma spraying method.

1n 1986, Browning Engineering Company invented a supersonic plasma spraying system named "PlazJet" [6]. Hybridizing high voltage extended arc plasma with high gas acceleration in an extended nozzle, which led to gas velocity in a supersonic mode at the nozzle exit with high arc power. However, the disadvantage of "PlazJet" was the high energy (up to 270 kW) and gas flow consumption during plasma spraying, which resulted in a very high product cost. Recently, an advanced high efficiency supersonic plasma spraying system (SAPS) has been successfully developed by national key laboratory for remanufacturing (China) for the deposition of ceramic and metallic coatings with good performance while the energy consumption was greatly reduced (lower than 80 kW) as compared with "PlazJet" [7,8].

Therefore, in the present study, TBCs were prepared by high efficiency supersonic atmospheric plasma spraying. The microstructure and mechanical properties of as-sprayed coating were studied with the aim of obtaining high-performance TBCs.

Disc substrates used for supersonic plasma sprayed YSZ-based TBCs were made of a nickel-base superalloy, GH3030 with nominal composition of Cr-22, Ti-0.35, Fe ≤ 1.5, C ≤ 0.12, Mn ≤ 0.7, Si ≤ 0.8, Al ≤ 0.15, Ni-balance (wt.%). The samples with a diameter of 20 mm and a thickness of 10 mm were used for thermal shock resistance test. All the substrates were degreased ultrasonically in acetone and then blasted with alumina grit before spraying. The commercially available CoNiCrAlY powder (AMDRY 995M, Sulzer Metco Inc. USA) with nominal composition of Ni-32, Cr-21, Al-8, Y-0.4, Co-balance (wt.%) with average particle size about 65 μm, as shown in Fig. 1a, was used for spraying the bond coat. The commercial spherical 8 wt.% YSZ powders (SY-133, Sang Rao Technical Co., Ltd., China) with particle size 10–45 μm, as shown in Fig. 1b, were used for spraying the top ceramic coat. Both the bond coat and top coat were deposited by high efficiency supersonic atmospheric

* Corresponding authors. State Key Laboratory for Mechanical Behavior of Materials, Xi'an Jiaotong University, Xi'an 710049, China. Tel.: +86 29 82668614; fax: +86 29 82663453.
E-mail addresses: byxjtu@gmail.com (Y. Bai), zhhan1955@163.com (Z.H. Han).

0042-207X/$ – see front matter
http://dx.doi.org/10.1016/j.vacuum.2013.05.013

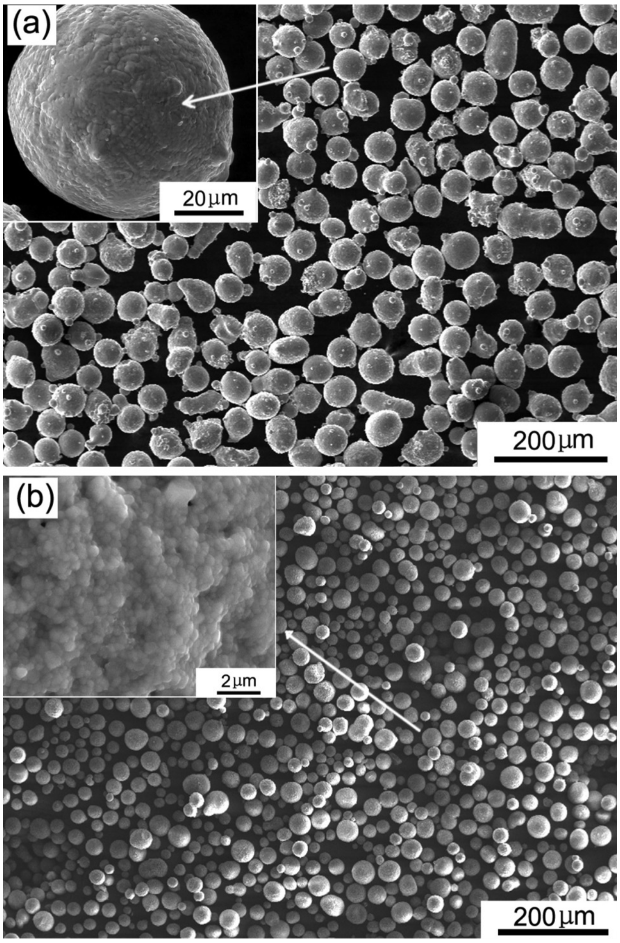

Fig. 1. Morphology of original feedstock powders: (a) SEM image of CoNiCrAlY powder, (b) SEM image of YSZ powder.

plasma spraying (SAPS) system. The keys of this system were a novel SAPS gun and powder injection, which was internal to the torch and directed perpendicular to the plasma flow and parallel to the torch trajectory. Details of the spraying parameters were listed in Table 1.

The microstructures of the samples were determined by scanning electron microscope (VEGAII XMU, Tescan, Czech Republic) and transmission electron microscope (JSM-6700F, JEOL, Japan). Porosity of the coatings was estimated by quantitative image analysis (IA) using a picture analysis system in scanning electron microscope (SEM) and 15 fields were selected for the measurement

Table 1
Spray parameters for CoNiCrAlY and YSZ powders.

Parameters	CoNiCrAlY	YSZ
Gun nozzle inner diameter (mm)	6	6
Powder injection port inlet diameter (mm)	2	2
Current (A)	363	405
Voltage (V)	124	160
Primary gas Ar (slpm)	65	60
Second gas H_2 (slpm)	8	17
Carrier argon gas flow rate (slpm)	8	7.5
Gun traverse speed (mm/s)	800	800
Powder feed rate (g/min)	40	40
Spray distance (mm)	100	100

* It was noted that the powder injection port was inside the nozzle and positioned at a distance of 12 mm from the nozzle outlet.

of porosity. The bonding strength of the as-sprayed coatings was measured using a materials tester (Instron1196, USA) in accordance with ASTM C 633-79 standard. Nickel-base superalloy, GH3030, rod was used as the substrate with diameter of 25.4 mm. Film epoxy adhesive (FM-1000, USA) with tensile fracture strength more than 60 MPa was applied. The final value represented the average of 5 samples sprayed at the same parameters. In order to determine the fracture toughness of coatings, Vickers indentations were also performed on polish cross-sections using a hardness tester. The indentation load was 5 N. Both Vickers diagonals and crack lengths were measured by SEM. The fracture toughness of as-sprayed coatings was calculated by the following equations [9]:

$$K_C = 0.203(c/a)^{-3/2}\mathrm{HV}_p a^{1/2} \quad (1)$$

where HV_p is the Vickers hardness, a is the half of the average length of two indents diagonal and c is the half of average crack length.

Thermal shock tests were conducted by using a muffle furnace. When the temperature inside the furnace reached approximately 1100 °C, the samples were directly inserted into the furnace holding for 5 min and then water quenching. The water temperature throughout the cycling was between 20 and 30 °C by continuously adding the cool water. When a visible spalled area of the surface of the top YSZ coating (quantitatively calculated by image analysis software Image Tool 3.0) reached about 10% of the total area, cycling was stopped and the number of thermal cycles was recorded.

Fig. 2 shows the microstructure of the coating fabricated by SAPS. As shown in Fig. 2a, the micro-pores were homogeneously distributed in the coating and no obvious cracks were observed at the interface of the top coat and bond coat. The porosity of the as-sprayed coating was approximately 3 % measured by quantitative image analysis. The above result indicated that the SAPS-coating had a denser microstructure and less irregular inter-splat pores and cracks than the previously reported conventional atmospheric plasma sprayed coatings [10–12]. Meanwhile, as seen in Fig. 2b, the as-sprayed coating was composed of well-adhered lamellar structures (splats). The columnar grain structure within the individual splats was visible because rapid nucleation occurred at the cooler surface of the flattened droplet at large under-cooling and the crystals grew rapidly opposite to the heat flow, forming a columnar grain structure. In addition, the TEM images (as shown in Fig. 2c and d) indicated that the size of columnar grain structure was in the range from 200 to 500 nm and some micro-pores existed between the splats.

Fig. 3 shows the morphology of Vickers indentation on the polished cross-section of as-sprayed coating. Both Vickers diagonals and crack lengths were measured in the SEM images. As shown in Fig. 3, the generation and propagation of crack was along both Vickers vertical and horizontal diagonals instead of only horizontal diagonals, which was similar with the way of crack propagation in the bulk ceramic material. The K_{IC} of the SAPS-coatings was 3.7 ± 0.4 MPa $m^{1/2}$. This value was between the conventional APS-coatings (2.7 ± 0.4 MPa $m^{1/2}$) and bulk YSZ materials (5.5 ± 0.3 MPa $m^{1/2}$) [13,14]. The result indicated that YSZ coating deposited by SAPS had higher crack propagation resistance ability than that of the conventional atmospheric plasma spraying. In addition, the bonding strength (between the top coat and bond coat) of SAPS-coating was 52 ± 4 MPa according to ASTM C 633-79 standard. During the bonding strength measurements, the samples fractured along the top coat/bond coat interface and the failures were referred to as *black fracture* [15]. The microstructure of the as-sprayed coating was strongly dependent on the interaction of molten droplets with the underlying surface [16]. The flattening degree, defined as the ratio of splat diameter to impacting droplet